HHS Public Access

Author manuscript

Thromb Haemost. Author manuscript; available in PMC 2018 December 06.

Published in final edited form as:

Thromb Haemost. 2017 December ; 117(12): 2322–2333. doi:10.1160/TH17-06-0433.

Developmental Stage-Specific Manifestations of Absent TPO/c-MPL Signalling in Newborn Mice

Viola Lorenz[1,*], **Haley Ramsey**[1,*], **Zhi-Jian Liu**[1], **Joseph Italiano Jr.**[2], **Karin Hoffmeister**[2,3], **Sihem Bihorel**[4,5], **Donald Mager**[4], **Zhongbo Hu**[6], **William B. Slayton**[6], **Benjamin T. Kile**[7,8], **Martha Sola-Visner**[1,*], and **Francisca Ferrer-Marin**[1,9,*]

[1]Division of Newborn Medicine, Boston Children's Hospital, Harvard Medical School, Boston, MA

[2]Hematology Division, Brigham and Women's Hospital, Harvard Medical School, Boston, MA

[3]Blood Center of Wisconsin, WI

[4]Department of Pharmaceutical Sciences, University of Buffalo, State University of New York, Buffalo, NY

[5]Center for Pharmacometrics and Systems Pharmacology, Orlando FL

[6]Department of Pediatrics, University of Florida, Gainesville, FL

[7]The Walter and Eliza Hall Institute of Medical Research, Parkville, Victoria, Australia

[8]Department of Anatomy and Developmental Biology, Monash Biomedicine Discovery Institute, Monash University, Melbourne, Australia

[9]Unidad de Hematología y Oncología Médica, Hospital Morales-Meseguer, Centro de Hemodonacion, IMIB-Murcia, CIBERER (CB15/00055), UCAM, Spain

Abstract

Congenital amegakaryocytic thrombocytopenia (CAMT) is a disorder caused by c-MPL mutations that impair thrombopoietin (TPO) signalling, resulting in a near-absence of megakaryocytes (MKs). While this phenotype is consistent in adults, neonates with CAMT can present with severe thrombocytopenia despite normal MK numbers. To investigate this, we characterized MKs and platelets in newborn *c-MPL*$^{-/-}$ mice. Liver MKs in *c-MPL*$^{-/-}$ neonates were reduced in number and size compared to WT age-matched MKs, and exhibited ultrastructural abnormalities not found in adult *c-MPL*$^{-/-}$ MKs. Platelet counts were lower in *c-MPL*$^{-/-}$ compared to WT mice at birth and did not increase over the first two weeks of life. *In vivo* biotinylation revealed a significant

Address correspondence to: Martha Sola-Visner, MD; Boston Children's Hospital, Division of Newborn Medicine, 300 Longwood Avenue, Enders Research Building, Rm. 961, Boston, MA 02115, United States; Phone: 617-919-4845; Fax: 617-730-0260; Martha.Sola-Visner@childrens.harvard.edu.

*These authors contributed equally to this work

AUTORSHIP CONTRIBUTIONS

V.L., H.R, Z-J.L., S.B., D.M., Z.H. and F.F-M., designed and performed experiments, collected and analyzed data, and wrote the manuscript; J.I. Jr. performed and interpreted the electron microscopy studies; K.H., W.B.S. and B.T.K. assisted with experimental design, data interpretation, and preparation of the manuscript; M.S-V. and F.F-M supervised and designed experiments, interpreted data, and wrote the manuscript.

CONFLICT-OF-INTEREST DISCLOSURE

The authors declare no competing financial interests.

reduction in the platelet half-life of *c-MPL*$^{-/-}$ newborn mice (P2) compared to age-matched WT pups, which was not associated with ultrastructural abnormalities. Genetic deletion of the pro-apoptotic Bak did not rescue the severely reduced platelet half-life of *c-MPL*$^{-/-}$ newborn mice, suggesting that it was due to factors other than platelets entering apoptosis early. Indeed, adult GFP+ platelets transfused into thrombocytopenic *c-MPL*$^{-/-}$ P2 pups also had a shortened lifespan, indicating the importance of cell-extrinsic factors. In addition, neonatal platelets from WT and *c-MPL*$^{-/-}$ mice exhibited reduced P-selectin surface expression following stimulation compared to adult platelets of either genotype, and platelets from *c-MPL*$^{-/-}$ neonates exhibited reduced GPIIb/IIIa activation in response to thrombin compared to age-matched WT platelets. Taken together, our findings indicate that c-MPL deficiency is associated with abnormal maturation of neonatal MKs and developmental stage-specific defects in platelet function.

Keywords

Animal models; Bone marrow; Megakaryocytes; Platelet physiology; Thrombocytopenia

INTRODUCTION

Over the last decade, it has become increasingly clear that there are substantial developmental differences between fetal, neonatal, and adult megakaryocytes (MKs) and platelets (1–3). Recent studies have revealed that fetal/neonatal megakaryopoiesis is characterized by a unique pattern of rapid proliferation followed by full cytoplasmic maturation without polyploidization, which gives rise to large numbers of small, low-ploidy, but mature MKs (4). This process, different from adult megakaryopoiesis, is regulated by a developmental stage-specific interplay of pathways, and by changes in the MK transcriptome during ontogeny (4–7). The effects of these cellular and molecular differences on *in vivo* physiological and pathological megakaryopoiesis and platelet homeostasis have not been investigated.

Understanding the developmental differences in MK and platelet biology is critical to elucidate the pathogenesis of a number of MK disorders that present with developmental stage-specific clinical manifestations, such as the transient myeloproliferative disorder associated with Down syndrome and GATA-1s mutations, the Thrombocytopenia Absent Radius (TAR) syndrome, which improves spontaneously after infancy, and Congenital Amegakaryocytic Thrombocytopenia (CAMT) (8–12). CAMT is a severe thrombocytopenic disorder characterized by the near absence of megakaryocytes (13, 14). It is caused by mutations in the gene encoding c-MPL, the receptor for thrombopoietin (TPO), which is the major megakaryocytic lineage growth factor. While its phenotype is consistent in adults, infants and children with CAMT can have near normal platelet counts during infancy and childhood (preceding the development of severe thrombocytopenia) (13, 15–18). Alternatively, CAMT patients have been described who, as neonates, presented with severe thrombocytopenia despite appropriate numbers of immature-appearing MKs in their bone marrow (BM), suggesting that mechanisms other than reduced megakaryopoiesis contributed to their thrombocytopenia in neonatal life (19–21).

Here, we used newborn and adult *c-MPL*$^{-/-}$ mice to systematically investigate the mechanisms underlying the thrombocytopenia associated with impaired TPO/c-MPL signalling at different developmental stages. Adult *TPO*$^{-/-}$ and *c-MPL*$^{-/-}$ mice exhibit an 85% reduction in MK numbers and platelet counts, but the residual MKs and platelets have been reported to be ultrastructurally and functionally normal (22–24). In contrast, we found that MKs in the liver of newborn *c-MPL*$^{-/-}$ mice (the primary hematopoietic site at birth) were less mature, and exhibited ultrastructural defects. Platelet counts at birth were significantly lower in *c-MPL*$^{-/-}$ pups relative to WT counterparts, and *in vivo* biotinylation studies demonstrated that platelet half-life in *c-MPL*$^{-/-}$ newborn pups was markedly reduced. The latter was not the result of accelerated entry into apoptosis, since deletion of pro-apoptotic Bak - the essential regulator of platelet life span - did not restore platelet survival kinetics in *c-MPL*$^{-/-}$ neonates to wild-type equivalency. Intriguingly, the reduction in platelet half-life appears to be cell-extrinsic. C-*MPL*$^{-/-}$ platelets from neonates exhibited a genotype-specific reduction in the surface expression of activated GPIIb/IIIa in response to thrombin, and neonatal platelets of either genotype exhibited a marked reduction in P-selectin surface expression following activation compared to adult platelets. C-*MPL*$^{-/-}$ platelets from adult mice also exhibited reduced P-selectin expression in response to stimulation compared to adult WT platelets, but not to the degree observed in neonates. Taken together, these observations demonstrate that TPO plays a role in neonatal MK maturation and has developmental stage-specific effects on platelet function.

METHODS

Animals

C57BL/6J mice were obtained from The Jackson Laboratory, Bar Harbor, ME. *c-MPL*$^{-/-}$ mice (22) were generously provided by Dr. William Slayton, *Bak*$^{-/-}$ mice by Dr. Loren Walensky, and *GFP+* mice by Dr. Karin Hoffmeister. Mice were maintained in a pathogen-free environment, and all studies were approved by the Boston Children's Hospital Animal Care and Use Committee.

Transmission electron microscopy (TEM)

Livers from WT and c-MPL$^{-/-}$ newborn mice (post-natal day 1 [P1] and P3) were processed as previously described (25). Briefly, livers were fixed in a mixture of paraformaldehyde and glutaraldehyde in 0.1 M Sodium Cacodylate Buffer, postfixed in 1% osmium tetroxide/1.5% potassium ferrocyanide (in H_2O), and embedded in Epon (EMbed 818) with propylene oxide. Ultrathin sections were obtained from areas previously identified to contain at least one MK by microscopic examination of semithin sections, and were stained with uranyl acetate and lead citrate prior to TEM. MKs were photographed on a Tecnai™ G^2 Spirit BioTWIN electron microscope (Hillsboro, OR) at an accelerating voltage of 80 kV. Images were recorded with an AMT 2k CCD camera (Danvers, MA). The ultrastructure of MKs was analyzed by three of the authors (F.F-M, J.I. and M.S-V) in a blinded fashion.

MKs were classified as immature, maturing and mature, using well established published criteria (26, 27). Stage I, or immature, MKs were recognized as small and round cells with a large nucleus, usually bilobed, lacking peripheral heterochromatin, and with prominent

nucleoli. At this stage, a few α-granules are present and serve to identify the cells as megakaryocytic. Stage II or maturing MKs contain a more lobulated nucleus, the DMS has begun to form, and α-granules are more numerous and homogeneously distributed in the cytoplasm. Stage III or mature MKs are bigger cells, in which the nucleus is pushed to one pole and nucleoli are rarely seen, granules are abundant in the cytoplasm, and the DMS is well developed and distributed throughout the cytoplasm.

Platelet Preparation for TEM

Whole blood was obtained from newborn (P2 and P5) mice by decapitation and bleeding into a tube containing 20 U/mL heparin. Platelet-rich plasma (PRP) was obtained by centrifugation at 300 g for 6 minutes at room temperature (RT). PRP was then centrifuged at 1000 g for 5 minutes and the pellet was pre-fixed in 0.1% glutaraldehyde for 10 min at 37°C and 1h at RT. Platelets were then again pelleted and fixed with a final concentration of 1.25 % paraformaldehyde, 2.5 % glutaraldehyde, 0.03 % picric acid and 0.1 M cacodylate buffer. Pellets were then processed for TEM as described above.

Histology

Murine liver and spleen samples were flash-frozen and cryosections were generated and fixed in 4% paraformaldehyde for 15 minutes. Unspecific binding sites were blocked and sections were stained with FITC-conjugated rat anti-mouse CD41 (clone: MWReg 30; BD Pharmingen, San Jose, CA) antibody and DAPI. Bones from adult mice were decalcified in 300 mM EDTA, fixed, paraffin-embedded, and sectioned. After antigen retrieval and blocking, MKs were stained with a rabbit anti-Von Willebrand Factor (vWF) antibody (DAKO, Denmark) and quantified using a microscope lens reticle (Klarmann Rulings, Inc) as described (28).

Murine blood sampling and analysis

Blood obtained by tail vein nick (adults) or by puncturing the anterior facial vein with a 30-gauge needle (neonates) was collected with a calibrated micropipette (5 μL) and immediately diluted in Cellpack (Sysmex, Kobe, Japan) supplemented with EDTA and PGE_1. Platelet counts, immature platelet fraction (IPF) and mean platelet volume (MPV) were measured on a Sysmex XT-2000i automatic haematology analyzer (Sysmex, Kobe, Japan). The immature platelet count (IPC) was calculated as the product of the IPF x platelet count.

Platelet lifespan

NHS-biotin solution (5 mg/ml) was infused in P2 and adult mice at a dose of 10 μL/g. Beginning at 1 hour post-infusion, blood was collected every 24 hours (2 μl). Blood samples were immediately diluted and incubated with FITC-conjugated anti-mouse CD41 (clone: MWReg30, BD Pharming, San Jose, CA) and PE-conjugated Avidin, and the percentage of biotinylated platelets was determined by flow cytometry. Total numbers of biotinylated platelets were calculated at each time point by multiplying platelet count x biotinylated platelet percentage x blood volume (70.5 μL/gram body weight), in order to account for the rapidly expanding blood volume in newborn mice (25). Data were then expressed as percent

change in total biotinylated platelets starting at 24 hours after biotinylation, as previously described (25).

Analysis of glycoprotein expression and platelet activation

Whole blood was obtained from adult mice by retroorbital bleeding and from newborn mice (P2 and P5) by decapitation and bleeding into a tube containing 20 U/mL heparin. For flow cytometric analysis of surface protein expression, platelets were stained for 15 min at RT with CD41-FITC (clone MWReg30; BD Pharming, San Jose, CA) or GPIbα-FITC (clone: Xia.G5; Emfret analytics, Eibelstadt, Germany). Subsequently, samples were quantified in a flow cytometer. To measure platelet activation the blood was washed twice in Ca^{2+}-free modified Tyrode's buffer containing apyrase (0.02 U/ml) and PGI_2 (0.1 μg/ml). Finally, the blood was resuspended in Ca^{2+}-containing modified Tyrode's buffer. The washed blood was left untreated or incubated with agonists at the indicated concentrations for 15 min in the presence of JON/A-PE (clone: JON/A, emfret analytics, Eibelstadt., Germany) and APC-conjugated anti-mouse P-selectin (clone: RB40.34; BD Pharming, San Jose, CA) antibody, followed by analysis on a FACS-Fortessa.

Platelet Bcl-xL levels

Bcl-xL concentrations in platelets were analyzed by intracellular flow cytometry as previously described (25).

Transfusion of GFP+ platelets

Whole blood was obtained from adult GFP+ mice by retroorbital bleeding and centrifuged twice at 800 rpm for 5 min to obtain PRP. To generate washed platelets, the PRP was centrifuged at 2,800 rpm for 5 min and the pellet was resuspended in 1 ml Ca^{2+}-free Tyrode's buffer. Adult *c-MPL*$^{-/-}$ mice were injected retroorbitally with a platelet suspension containing 2.5×10^9 platelets/mL, at a dose of 20 μL/g to correct the thrombocytopenia or 2 μL/g to follow the lifespan of the transfused platelets without substantially rising the platelet count. Because of the smaller blood volume of newborn (P2) pups, they were all transfused into the superficial temporal vein with 20 μL/g of a platelet suspension containing either 2.8×10^9/mL platelets (to correct the thrombocytopenia) or 0.7×10^9/mL (to track transfused platelets without correcting the thrombocytopenia). The GFP+ platelet percentage, platelet counts and body weights were monitored daily for 96 hours. Due to the rapid increase in body weight during early post-natal life, the absolute GFP+ platelet count was calculated daily accounting for changes in platelet count and blood volume, in a manner identical to biotinylated platelet counts. Changes in GFP+ platelets were expressed as percent changes from the initial count 2 hours after transfusion (set as 100%).

Statistical Analysis

Results from at least 3 experiments per group are presented as mean ± SEM, unless otherwise indicated. Differences between two groups were assessed by Student's-t-test (Excel). $P < 0.05$ was considered statistically significant.

RESULTS

c-MPL$^{-/-}$ newborn mice exhibit decreased MKs in liver and spleen

Since the liver is the main site of megakaryopoiesis in newborn mice, MKs (CD41+ cells) were evaluated in newborn livers of WT and *c-MPL*$^{-/-}$ mice by fluorescence microscopy (25, 28). MKs in neonatal (P2) *c-MPL*$^{-/-}$ liver sections were significantly reduced in number and size compared to WT mice (Figure 1A). At P2, the MK number in *c-MPL*$^{-/-}$ mice was 1.5±1.1 vs. 8.7±2.7 in WT mice, respectively ($p<0.001$).

By P5, the contribution of the liver to haematopoiesis had decreased sharply (Figure 1A), and the main site of megakaryopoiesis had become the spleen, while the BM remained hypocellular (25). Histological analysis of splenic tissue obtained from P2, P5, and adult mice revealed that, at all ages, CD41+ MKs were present in fewer numbers in *c-MPL*$^{-/-}$ compared to WT counterparts (Figure 1B). MKs were also present in lower numbers in the BM of adult *c-MPL*$^{-/-}$ compared to WT mice ($p<0.001$) (Figure 1C). In both *c-MPL*$^{-/-}$ and WT mice, MK size increased over time, but at all times and tissues *c-MPL*$^{-/-}$ MKs were smaller than their WT counterparts (Figure 1A–C).

c-MPL$^{-/-}$ MKs in the newborn liver are ultrastructurally abnormal

Next, we examined the ultrastructure of *c-MPL*$^{-/-}$ and WT newborn liver MKs by TEM. In WT newborn livers (n=4), 17 of the 32 (53%) MKs examined were maturing and 15 of 32 (47%) were mature, with abundant granules and a well-developed demarcation membrane system (DMS) (Figure 2A) (14). In contrast, in newborn *c-MPL*$^{-/-}$ livers (n=13), 6 of the 28 (22%) MKs found were immature (with a large nucleus and very few granules) (Figure 2B), 57% (16/28) were maturing with a developing DMS, and only 21% were mature. Furthermore, 19 of the 28 (68%) *c-MPL*$^{-/-}$ neonatal MKs exhibited ultrastructural abnormalities, not described in adult *c-MPL*$^{-/-}$ mice (24). These abnormalities were found at all stages of MK maturation and were primarily related to the DMS, which was poorly developed and disorganized (Figure 2C) or irregularly distributed throughout the cytoplasm (Figure 2D). Neonatal *c-MPL*$^{-/-}$ MKs also frequently exhibited an abnormally wide peripheral zone, without organelles or DMS (Figures 2C, E, F). Occasionally, they also displayed a persistent large central nucleus (Figure 2E) or a prominent nucleolus (Figure 2D).

Platelets in *c-MPL*$^{-/-}$ newborn mice have a markedly reduced half-life

Next, we evaluated platelet counts during the transition from neonatal to adult haematopoiesis. At P2, *c-MPL*$^{-/-}$ mice exhibited a mean platelet count of 170±54 $\times 10^3$/μl, 26% of that in age-matched WT mice (648±137 $\times 10^3$/μl). By P14, *c-MPL*$^{-/-}$ platelet counts remained stable (186±74 $\times 10^3$/μl), while WT platelet counts had nearly doubled, to 1,333±116 $\times 10^3$/μl (Figure 3A). Thus, by P14, platelet counts in *c-MPL*$^{-/-}$ mice were 10–15% of those in WT mice, similar to adults. Over the same period of life, the mean platelet volume (MPV) decreased in both WT and *c-MPL*$^{-/-}$ mice, although *c-MPL*$^{-/-}$ platelets were consistently larger. This difference was statistically significant during the first week of life (Figure 3B). In adult life, MPV was similar in *c-MPL*$^{-/-}$ and WT mice (6.4±0.4 vs. 6.5±0.2 fl; $p=0.94$).

The immature platelet fraction (IPF) is the percentage of platelets that have been newly released into the circulation, which are recognized by the presence of RNA. The IPF% decreased in WT mice during the first week of life, while it remained stable in *c-MPL*$^{-/-}$ mice on days P2 to P6 prior to decreasing on P8 (Supplemental Figure 1). There were no significant differences in IPF% between WT and *c-MPL*$^{-/-}$ mice at P2 and P4. The immature platelet count (IPC), which is calculated by multiplying platelet count x IPF%, indicates the number of newly released platelets in the circulation, and is a measure of platelet production (29). The IPC decreased in WT mice over the first week of life, stabilizing during the second week at a level similar to that of adult WT mice (Figure 3C). In contrast, the IPC in newborn *c-MPL*$^{-/-}$ mice was significantly lower ($p<0.001$) than that of WT, and remained relatively stable throughout the transition from neonatal to adult megakaryopoiesis, at levels similar to those of adult *c-MPL*$^{-/-}$ mice.

In WT mice, the rise in platelet counts that occurs during the first two weeks of life is associated with a transient prolongation of platelet lifespan (25). Since platelet counts did not increase in neonatal *c-MPL*$^{-/-}$ mice, we evaluated platelet survival *in vivo*. Of note, newborn and adult *c-MPL*$^{-/-}$ mice included in the biotinylation studies had similar degrees of thrombocytopenia (Figure 3D). These studies revealed a significantly shorter platelet half-life in P2 *c-MPL*$^{-/-}$ mice compared to their age-matched WT counterparts (34 ± 2 vs. 57 ± 5 hours, respectively; $p=0.001$), representing a 41% reduction (Figure 3E). A shorter platelet half-life was also observed in adult *c-MPL*$^{-/-}$ compared to WT animals (32 ± 3 vs. 44 ± 3 hours, respectively; $p<0.01$), although this reduction was of a lesser magnitude (28%) (Figure 3F).

Platelets from *c-MPL*$^{-/-}$ newborn pups exhibit normal ultrastructure and glycoprotein surface expression

Based on the presence of ultrastructural abnormalities in neonatal *c-MPL*$^{-/-}$ MKs, we next examined P2 *c-MPL*$^{-/-}$ platelets by TEM. Other than an increase in size, these platelets exhibited no substantial ultrastructural differences compared to age-matched WT platelets (Figure 4A). Neonatal (P2 and P5) WT platelets exhibited significantly higher GPIIb surface expression levels than adult platelets ($P<0.01$ for both), consistent with their larger size, although no differences were observed in GPIbα expression. There were no significant differences between WT and *c-MPL*$^{-/-}$ mice at P2, P5 or in adulthood (Figure 4B).

The attenuated lifespan of neonatal *c-MPL*$^{-/-}$ platelets is not due to decreased Bcl-xL levels, and is not corrected by Bak depletion

Adult platelet lifespan is controlled by the balance between the anti-apoptotic protein Bcl-xL (regulated by TPO) and the pro-apoptotic protein Bak. Loss of Bak almost doubles platelet lifespan in WT mice by inhibiting platelet apoptosis (30). We therefore measured Bcl-xL protein levels in WT and *c-MPL*$^{-/-}$ P2 platelets by intracellular flow cytometry. Cells of both genotypes exhibited similar Bcl-xL levels (data not shown), suggesting no imbalance in the intrinsic apoptosis pathway. To establish whether loss of Bak could normalize platelet lifespan in newborn *c-MPL*$^{-/-}$ mice, we generated *c-MPL*$^{-/-}$/*Bak*$^{-/-}$ double knockout mice and analyzed platelet counts and platelet lifespan. Mean platelet counts were not different in P2 *c-MPL*$^{-/-}$/*Bak*$^{+/+}$, *c-MPL*$^{-/-}$/*Bak*$^{+/-}$ and *c-MPL*$^{-/-}$/*Bak*$^{-/-}$ littermates (125±16, 108±10

and 130±19 × 10^3/μL, respectively). At P5, platelet counts remained similar in *c-MPL*$^{-/-}$/*Bak*$^{+/+}$, *c-MPL*$^{-/-}$/*Bak*$^{+/-}$ and *c-MPL*$^{-/-}$/*Bak*$^{-/-}$ mice (Figure 5A). In biotinylation studies, partial or complete loss of Bak did not rescue the striking reduction in platelet half-life (Figure 5B), which remained substantially shorter than the approximately 60 hours seen in WT neonates (Figure 3E). These observations indicated that the short half-life on neonatal *c-MPL*$^{-/-}$ platelets was due to reasons other than these platelets entering Bak-mediated apoptosis earlier.

Transfused adult platelets have reduced survival in thrombocytopenic *c-MPL*$^{-/-}$ neonatal mice

Next, we examined whether cell-extrinsic mechanisms might underpin the rapid platelet clearance observed in newborn *c-MPL*$^{-/-}$ mice. To test this, we transfused P2 and adult *c-MPL*$^{-/-}$ mice with platelets from adult mice expressing GFP in all hematopoietic cells, including platelets. We adjusted the number of transfused platelets to either maintain the thrombocytopenia ("low group") or to increase the platelet count to near-normal levels ("high group") (Figure 6A). We then tracked the survival of transfused GFP+ platelets in the circulation, accounting for changes in blood volume in neonates, as described.(25) Interestingly, the half-life of adult GFP+ platelets was significantly shorter in newborn thrombocytopenic (low group) mice (29 ± 6 hours) compared to pups whose platelet count had been normalized by transfusion (high group; 52 ± 3 hours, $p<0.01$ vs. low group) (Figure 6B). In contrast, there were no significant differences in the half-life of transfused platelets between adult *c-MPL*$^{-/-}$ mice in the low and high groups (43 ± 5 vs. 54 ± 3 hours, respectively; $p=0.15$) (Figure 6C). These results demonstrated that cell-extrinsic mechanisms contribute to the rapid platelet clearance in newborn mice with mild to moderate levels of thrombocytopenia.

C-MPL$^{-/-}$ platelets have developmental stage- and genotype-specific functional defects

Collectively, our data indicated that cell-extrinsic factors (rather than early entry into apoptosis) are the primary reason platelet half-life is markedly reduced in *c-MPL*$^{-/-}$ newborns. To explore whether platelet functional defects in neonatal *c-MPL*$^{-/-}$ platelets contributed to the accelerated platelet consumption, we evaluated agonist-induced activation of GPIIb/IIIa (JON/A) and P-selectin exposure in P2, P5, and adult *c-MPL*$^{-/-}$ and WT platelets. Incubation of newborn and adult WT platelets with thrombin (0.1 U/ml) led to GPIIb/IIIa activation in >80% of WT platelets at all stages of development (Figures 7A, B). However, the percentage of platelets activated in response to thrombin was significantly lower in newborn (P2 and P5) *c-MPL*$^{-/-}$ vs. age-matched WT mice, a difference not found in adults (Figure 7B). These genotype-dependent differences were also found when the response to stimulation was measured as fold change in mean fluorescent intensity (MFI) between activated and resting platelets (Figure 7C). This did not appear to be the result of a global platelet activation defect, since neonatal and adult WT and *c-MPL*$^{-/-}$ platelets exhibited similar JON/A MFI fold changes in response to stimulation with ADP and the thromboxane agonist U46619 (Supplemental Figure 2A–C).

Next, we analyzed P-selectin exposure, a measure of activation-induced platelet degranulation, in response to thrombin stimulation. These studies revealed striking

developmental differences in P-selectin surface expression following thrombin stimulation, with both the percentage of P-selectin positive platelets and particularly the MFI fold change increasing with advancing post-natal age in WT and *c-MPL*$^{-/-}$ mice (MFI fold change: WT P2 vs adult p<0.001, WT P5 vs adult p<0.001, *C-MPL*$^{-/-}$ P2 vs adult p<0.001, *c-MPL*$^{-/-}$ P5 vs adult p<0.001, Figures 7D, E and F). In addition to the striking developmental differences, *c-MPL*$^{-/-}$ adult mice exhibited significantly reduced P-selectin exposure (expressed as MFI fold-change) in response to stimulation, compared to their age-matched WT counterparts (Figure 7D, F; Supplemental Figure 2 F). Statistically significant differences in P-selectin expression were also observed between *c-MPL*$^{-/-}$ and WT P2 and P5 neonates upon stimulation with different agonists (Supplemental Figure 2D–F), but these were inconsistent and of questionable physiological relevance given the overall low P-selectin expression levels found in stimulated neonatal platelets of both genotypes.

DISCUSSION

Here we evaluated MK numbers, MK maturation, and platelet lifespan in newborn *c-MPL*$^{-/-}$ mice, to determine the mechanisms contributing to the thrombocytopenia associated with absent TPO signalling during neonatal life. Applying a combination of immunofluorescence and TEM, we demonstrated that MKs in the liver of newborn *c-MPL*$^{-/-}$ mice were smaller, more immature and exhibited significant ultrastructural abnormalities compared to neonatal WT MKs. These findings supported and expanded the recent observation from Potts *et al.*, who found an arrest in polyploidization at the 8N stage in *c-MPL*$^{-/-}$ fetal liver MKs at embryonic day 16.5 (E16.5) (31). Collectively, both studies conclusively demonstrate that the TPO/*c-MPL* axis is essential for the normal terminal differentiation of late fetal and neonatal MKs, in stark contrast to adult MKs, which mature normally in the absence of TPO or *c-MPL* (20, 32).

In addition to these maturational defects, we also found a reduction in the number of MKs present in the liver of neonatal *c-MPL*$^{-/-}$ compared to WT mice, indicating that the requirement of TPO for maintenance of MK numbers appears during late fetal life (31). In early murine embryonic life, platelets are produced by *c-MPL*-independent diploid platelet-forming cells (31). Between E14.5 and E16.5, *c-MPL*$^{-/-}$ fetuses exhibit normal numbers of low-ploidy MKs (contrasting with the high ploidy WT liver MKs), indicating a developmental-stage specific requirement of *c-MPL* signalling for terminal MK maturation, but not proliferation. At the time of birth, the presence of decreased numbers of immature or abnormally maturing MKs in *c-MPL*$^{-/-}$ livers likely reflects a temporal overlap between the effects of absent *c-MPL* signalling on prenatal and postnatal megakaryopoiesis.

Next, we examined serial platelet counts over the first two weeks of life in *c-MPL*$^{-/-}$ and WT mice. As previously described, WT mice nearly doubled their platelet counts during the second week of life, an increase that has been associated with a transient prolongation of the neonatal platelet lifespan (7). *c-MPL*$^{-/-}$ newborn mice, in contrast, did not increase their platelet counts, and exhibited a substantially shorter platelet half-life than WT pups. Adult *c-MPL*$^{-/-}$ mice also displayed a shorter platelet half-life than adult WT mice, but to a lesser degree than newborn mice. Importantly, *c-MPL*$^{-/-}$ mice can present two distinct phenotypes: one with extremely low platelet counts, approaching 3% of normal, and another with platelet

counts approximately 14% of normal (33, 34). Our study only included *c-MPL*$^{-/-}$ mice in the latter category. The mild reduction in the platelet half-life of our adult animals was consistent with two prior studies, but was quite different from the more severe reduction observed in newborn pups (33, 34).

Platelet lifespan is primarily regulated by the balance between anti-apoptotic and pro-apoptotic Bcl-2 protein family members, particularly Bcl-xL (which is regulated by TPO in megakaryoblastic cells) and Bak, respectively (35–38). Genetic or pharmacological Bcl-xL inhibition leads to a reduction in platelet survival. Correspondingly, genetic deletion of the pro-apoptotic Bak prolongs the platelet lifespan and increases platelet counts in WT and Bcl-xL$^{+/-}$ mice (30, 39). However, Bak deletion did not rescue the striking reduction in platelet half-life observed in *c-MPL*$^{-/-}$ mice, indicating that cell-extrinsic factors, rather than early entry into apoptosis, were responsible for the short platelet half-life in *c-MPL*$^{-/-}$ newborn mice.

In a recent study, Lebois *et al.* demonstrated that platelet survival in adult *c-MPL*$^{-/-}$ was shortened as a consequence of the thrombocytopenia, rather than as a result of the lack of *c-MPL* signalling on MKs and platelets (33). Consistent with a prior study, these investigators observed that adult *c-MPL*$^{-/-}$ mice with extremely low platelet counts (3% of normal) had shorter platelet survival than those with less severe thrombocytopenia, which was explained by microscopic bleeding (34). In the mice with less severe thrombocytopenia, however, no bleeding would be expected based on the severity of thrombocytopenia, and the reason for their reduced platelet survival remained unclear (40). One hypothesis is that a certain number of platelets are required daily to maintain hemostasis and prevent bleeding. In humans, approximately 7,000 platelets/μL are required daily to maintain hemostasis (41). This number, relatively insignificant in the setting of normal platelet counts, represents an increasingly larger fraction of the platelet count in the presence of thrombocytopenia, which shortens platelet survival as platelets are consumed prior to entering apoptosis. Modeling studies have suggested a higher fixed platelet requirement for mice than humans, but the exact number has not been determined (42). Our finding that newborn *c-MPL*$^{-/-}$ mice had substantially shorter platelet survival than adult *c-MPL*$^{-/-}$ mice with comparable degrees of thrombocytopenia suggested that newborn mice might have a higher daily fixed platelet requirement or might be more predisposed to microscopic bleeding than adult mice, or both.

The finding that transfused adult platelets had a significantly reduced lifespan in newborn pups when the post-transfusion platelet counts remained low, but not when the thrombocytopenia was corrected by the transfusion, supports the hypothesis that cell-extrinsic factors account for the accelerated platelet consumption during neonatal thrombocytopenia. In that regard, structural and functional animal studies have shown that neonates have a more fragile vasculature than adults, consistent with the active angiogenesis and vasculogenesis associated with the rapid growth during this developmental period (43, 44). Thus, it is likely that more platelets are required to maintain the integrity of these newly formed neonatal vessels, which might also predispose thrombocytopenic neonates to microscopic bleeding.

We also investigated the possibility of platelet functional defects, which could further contribute to the short platelet half-life observed during thrombocytopenia in *c-MPL*$^{-/-}$ mice, particularly during neonatal life. Similar to human reports, we found a striking decrease in the surface expression levels of P-selectin in neonatal platelets following stimulation by all agonists tested, independent of the genotype (45). P-selectin expression on the platelet surface is a marker of platelet degranulation, but it is unclear if our findings reflect a neonatal platelet degranulation defect and/or developmental differences in murine platelet P-selectin expression levels, which have been recently reported (46, 47). Interestingly, we also found a significant reduction in P-selectin exposure in response to stimulation in *c-MPL*$^{-/-}$ adult mice compared to their age-matched WT counterparts. Nevertheless, adult *c-MPL*$^{-/-}$ platelets still displayed significantly higher P-selectin levels upon stimulation than *c-MPL*$^{-/-}$ P2 or P5 platelets, indicating a more profound platelet functional defect in the neonates. Decreased P-selectin expression (in P-selectin$^{-/-}$ adult mice) does not affect the platelet lifespan in mice with normal platelet counts (48), but it is associated with defects in hemostasis, including a mild prolongation of the bleeding time and increased haemorrhage in inflammatory situation (49). The effects of P-selectin deficiency in the setting of thrombocytopenia have not been investigated, but it is plausible that reduced levels of P-selectin in thrombocytopenic *c-MPL*$^{-/-}$ mice could increase the risk of microscopic bleeding and contribute to the shortened platelet half-life.

The severely reduced P-selectin expression in neonatal platelets was not the result of a global platelet activation defect, since neonatal WT platelets exhibited a normal to mildly reduced conformational change of GPIIb/IIIa (measured by JON/A binding) in response to thrombin. However, we found decreased GPIIb/IIIa activation in thrombin-stimulated neonatal *c-MPL*$^{-/-}$ compared to age-matched WT platelets, a difference not present in adult mice. The reasons for this are unclear, but it is important to recognize that P2 platelets are almost entirely produced by fetal liver MKs, while P5 platelets reflect mostly splenic and adult platelets BM megakaryopoiesis. It is likely that their functional profiles reflect these different origins. We also recognize the possibility of additional developmental stage- or genotype-dependent differences in response to agonists we did not investigate, such as collagen or rhodocytin. Finally, it is possible that the loss of c-MPL in neonatal megakaryocytes/platelets directly affects neonatal platelet lifespan through other mechanisms, such as by altering platelet glycan composition. Studies transfusing neonatal *c-MPL*$^{-/-}$ platelets into WT newborn pups would be desirable but are not feasible, as they would require a large number of pups for a single transfusion and WT and *c-MPL*$^{-/-}$ litters to be born at the same time. Nevertheless, collectively our data strongly suggest that the more substantial reduction in platelet half-life observed in *c-MPL*$^{-/-}$ newborn mice is due to cell-extrinsic factors (i.e. a more fragile neonatal vasculature) and defects in platelet function that are more severe in neonates compared to adults. Our findings are likely to have relevance to our understanding of thrombocytopenia in human neonates, who also have platelet functional defects and a higher bleeding risk than older children or adults (50).

Supplementary Material

Refer to Web version on PubMed Central for supplementary material.

Acknowledgments

This work was supported by the National Institutes of Health Grants RO1 HL069990 (to M.S-V), HL046925, and by Grant P14/01956 from the Instituto de Salud Carlos III (to F.F-M).

This work was supported by the National Institutes of Health Grants RO1 HL069990 (to M.S-V), HL046925, and by Grant P14/01956 from the Instituto de Salud Carlos III (to F.F-M). The Sysmex XT-2000i automatic haematology analyzer used in this study was generously provided on an on-loan basis from Sysmex, Kobe, Japan.

References

1. Sola MC, Du Y, Hutson AD, et al. Dose-response relationship of megakaryocyte progenitors from the bone marrow of thrombocytopenic and non-thrombocytopenic neonates to recombinant thrombopoietin. Br J Haematol. 2000; 110(2):449–53. [PubMed: 10971407]
2. Pastos KM, Slayton WB, Rimsza LM, et al. Differential effects of recombinant thrombopoietin and bone marrow stromal-conditioned media on neonatal versus adult megakaryocytes. Blood. 2006; 108(10):3360–2. [PubMed: 16888093]
3. Liu ZJ, Sola-Visner M. Neonatal and adult megakaryopoiesis. Current opinion in hematology. 2011; 18(5):330–7. [PubMed: 21738028]
4. Liu ZJ, Italiano J Jr, Ferrer-Marin F, et al. Developmental differences in megakaryocytopoiesis are associated with up-regulated TPO signaling through mTOR and elevated GATA-1 levels in neonatal megakaryocytes. Blood. 2011; 117(15):4106–17. [PubMed: 21304100]
5. Klusmann JH, Godinho FJ, Heitmann K, et al. Developmental stage-specific interplay of GATA1 and IGF signaling in fetal megakaryopoiesis and leukemogenesis. Genes Dev. 2010; 24(15):1659–72. [PubMed: 20679399]
6. Woo AJ, Wieland K, Huang H, et al. Developmental differences in IFN signaling affect GATA1s-induced megakaryocyte hyperproliferation. J Clin Invest. 2013
7. Bluteau O, Langlois T, Rivera-Munoz P, et al. Developmental changes in human megakaryopoiesis. Journal of thrombosis and haemostasis : JTH. 2013; 11(9):1730–41. [PubMed: 23782903]
8. Majewski IJ, Metcalf D, Mielke LA, et al. A mutation in the translation initiation codon of Gata-1 disrupts megakaryocyte maturation and causes thrombocytopenia. Proc Natl Acad Sci U S A. 2006; 103(38):14146–51. [PubMed: 16966598]
9. Hollanda LM, Lima CS, Cunha AF, et al. An inherited mutation leading to production of only the short isoform of GATA-1 is associated with impaired erythropoiesis. Nat Genet. 2006; 38(7):807–12. [PubMed: 16783379]
10. Letestu R, Vitrat N, Masse A, et al. Existence of a differentiation blockage at the stage of a megakaryocyte precursor in the thrombocytopenia and absent radii (TAR) syndrome. Blood. 2000; 95(5):1633–41. [PubMed: 10688818]
11. al-Jefri AH, Dror Y, Bussel JB, et al. Thrombocytopenia with absent radii: frequency of marrow megakaryocyte progenitors, proliferative characteristics, and megakaryocyte growth and development factor responsiveness. Pediatr Hematol Oncol. 2000; 17(4):299–306. [PubMed: 10845228]
12. Dreyfus M, Tchernia G. Thrombocytopenia with absent radii (TAR syndrome): new advances in the mechanism of thrombocytopenia. Pediatr Hematol Oncol. 2000; 17(7):521–2. [PubMed: 11033726]
13. Ballmaier M, Germeshausen M, Schulze H, et al. c-mpl mutations are the cause of congenital amegakaryocytic thrombocytopenia. Blood. 2001; 97(1):139–46. [PubMed: 11133753]
14. Geddis AE. Congenital amegakaryocytic thrombocytopenia and thrombocytopenia with absent radii. Hematol Oncol Clin North Am. 2009; 23(2):321–31. [PubMed: 19327586]
15. Stoddart MT, Connor P, Germeshausen M, et al. Congenital amegakaryocytic thrombocytopenia (CAMT) presenting as severe pancytopenia in the first month of life. Pediatr Blood Cancer. 2013; 60(9):E94–6. [PubMed: 23625800]
16. Ihara K, Ishii E, Eguchi M, et al. Identification of mutations in the c-mpl gene in congenital amegakaryocytic thrombocytopenia. Proc Natl Acad Sci U S A. 1999; 96(6):3132–6. [PubMed: 10077649]

17. Germeshausen M, Ballmaier M, Welte K. MPL mutations in 23 patients suffering from congenital amegakaryocytic thrombocytopenia: the type of mutation predicts the course of the disease. Hum Mutat. 2006; 27(3):296.
18. King S, Germeshausen M, Strauss G, et al. Congenital amegakaryocytic thrombocytopenia: a retrospective clinical analysis of 20 patients. Br J Haematol. 2005; 131(5):636–44. [PubMed: 16351641]
19. Fox NE, Chen R, Hitchcock I, et al. Compound heterozygous c-Mpl mutations in a child with congenital amegakaryocytic thrombocytopenia: functional characterization and a review of the literature. Experimental hematology. 2009; 37(4):495–503. [PubMed: 19302922]
20. Rose MJ, Nicol KK, Skeens MA, et al. Congenital amegakaryocytic thrombocytopenia: the diagnostic importance of combining pathology with molecular genetics. Pediatr Blood Cancer. 2008; 50(6):1263–5. [PubMed: 18240171]
21. Henter JI, Winiarski J, Ljungman P, et al. Bone marrow transplantation in two children with congenital amegakaryocytic thrombocytopenia. Bone marrow transplantation. 1995; 15(5):799–801. [PubMed: 7670411]
22. Gurney AL, Carver-Moore K, de Sauvage FJ, et al. Thrombocytopenia in c-mpl-deficient mice. Science. 1994; 265(5177):1445–7. [PubMed: 8073287]
23. Alexander WS, Roberts AW, Nicola NA, et al. Deficiencies in progenitor cells of multiple hematopoietic lineages and defective megakaryocytopoiesis in mice lacking the thrombopoietic receptor c-Mpl. Blood. 1996; 87(6):2162–70. [PubMed: 8630375]
24. Bunting S, Widmer R, Lipari T, et al. Normal platelets and megakaryocytes are produced in vivo in the absence of thrombopoietin. Blood. 1997; 90(9):3423–9. [PubMed: 9345025]
25. Liu ZJ, Hoffmeister KM, Hu Z, et al. Expansion of the neonatal platelet mass is achieved via an extension of platelet lifespan. Blood. 2014; 123(22):3381–9. [PubMed: 24599546]
26. Bentfeld-Barker ME, Bainton DF. Ultrastructure of rat megakaryocytes after prolonged thrombocytopenia. J Ultrastruct Res. 1977; 61(2):201–14. [PubMed: 915981]
27. Poujol C, Ware J, Nieswandt B, et al. Absence of GPIbalpha is responsible for aberrant membrane development during megakaryocyte maturation: ultrastructural study using a transgenic model. Experimental hematology. 2002; 30(4):352–60. [PubMed: 11937271]
28. Hu Z, Slayton WB, Rimsza LM, et al. Differences between newborn and adult mice in their response to immune thrombocytopenia. Neonatology. 2010; 98(1):100–8. [PubMed: 20134184]
29. Sparger KA, Ramsey H, Lorenz V, et al. Developmental differences between newborn and adult mice in response to romiplostim. Platelets. 2017:1–8.
30. Josefsson EC, James C, Henley KJ, et al. Megakaryocytes possess a functional intrinsic apoptosis pathway that must be restrained to survive and produce platelets. J Exp Med. 2011; 208(10):2017–31. [PubMed: 21911424]
31. Potts KS, Sargeant TJ, Dawson CA, et al. Mouse prenatal platelet-forming lineages share a core transcriptional program but divergent dependence on MPL. Blood. 2015
32. Ng AP, Kauppi M, Metcalf D, et al. Mpl expression on megakaryocytes and platelets is dispensable for thrombopoiesis but essential to prevent myeloproliferation. Proc Natl Acad Sci U S A. 2014; 111(16):5884–9. [PubMed: 24711413]
33. Lebois M, Dowling MR, Gangatirkar P, et al. Regulation of platelet lifespan in the presence and absence of thrombopoietin signaling. Journal of thrombosis and haemostasis : JTH. 2016; 14(9): 1882–7. [PubMed: 27344013]
34. Coupland LA, Cromer D, Davenport MP, et al. A novel fluorescent-based assay reveals that thrombopoietin signaling and Bcl-X(L) influence, respectively, platelet and erythrocyte lifespans. Experimental hematology. 2010; 38(6):453–61e1. [PubMed: 20298742]
35. Zhang H, Nimmer PM, Tahir SK, et al. Bcl-2 family proteins are essential for platelet survival. Cell Death Differ. 2007; 14(5):943–51. [PubMed: 17205078]
36. Debrincat MA, Josefsson EC, James C, et al. Mcl-1 and Bcl-x(L) coordinately regulate megakaryocyte survival. Blood. 2012; 119(24):5850–8. [PubMed: 22374700]
37. Kodama T, Hikita H, Kawaguchi T, et al. Mcl-1 and Bcl-xL regulate Bak/Bax-dependent apoptosis of the megakaryocytic lineage at multistages. Cell Death Differ. 2012; 19(11):1856–69. [PubMed: 22790873]

38. Kirito K, Watanabe T, Sawada K, et al. Thrombopoietin regulates Bcl-xL gene expression through Stat5 and phosphatidylinositol 3-kinase activation pathways. J Biol Chem. 2002; 277(10):8329–37. [PubMed: 11756417]
39. Mason KD, Carpinelli MR, Fletcher JI, et al. Programmed anuclear cell death delimits platelet life span. Cell. 2007; 128(6):1173–86. [PubMed: 17382885]
40. Morowski M, Vogtle T, Kraft P, et al. Only severe thrombocytopenia results in bleeding and defective thrombus formation in mice. Blood. 2013; 121(24):4938–47. [PubMed: 23584880]
41. Hanson SR, Slichter SJ. Platelet kinetics in patients with bone marrow hypoplasia: evidence for a fixed platelet requirement. Blood. 1985; 66(5):1105–9. [PubMed: 4052629]
42. Dowling MR, Josefsson EC, Henley KJ, et al. A model for studying the hemostatic consumption or destruction of platelets. PloS one. 2013; 8(3):e57783. [PubMed: 23505441]
43. Ballabh P. Intraventricular hemorrhage in premature infants: mechanism of disease. Pediatric research. 2010; 67(1):1–8. [PubMed: 19816235]
44. Fu Z, Heldt GP, West JB. Increased fragility of pulmonary capillaries in newborn rabbit. Am J Physiol Lung Cell Mol Physiol. 2003; 284(5):L703–9. [PubMed: 12676761]
45. Sola-Visner M. Platelets in the neonatal period: developmental differences in platelet production, function, and hemostasis and the potential impact of therapies. Hematology / the Education Program of the American Society of Hematology American Society of Hematology Education Program. 2012; 2012:506–11.
46. Stolla MC, Leyens K, Catherman SC, et al. P-Selectin Expression and Platelet Function Are Developmentally Regulated. Blood. 2014; 124(21):1439.
47. Margraf A, Nussbaum C, Rohwedder I, et al. Maturation of Platelet Function During Murine Fetal Development In Vivo. Arterioscler Thromb Vasc Biol. 2017; 37(6):1076–86. [PubMed: 28428216]
48. Berger G, Hartwell DW, Wagner DD. P-Selectin and platelet clearance. Blood. 1998; 92(11):4446–52. [PubMed: 9834252]
49. Subramaniam M, Frenette PS, Saffaripour S, et al. Defects in hemostasis in P-selectin-deficient mice. Blood. 1996; 87(4):1238–42. [PubMed: 8608210]
50. Sparger KA, Assmann SF, Granger S, et al. Platelet Transfusion Practices Among Very-Low-Birth-Weight Infants. JAMA pediatrics. 2016

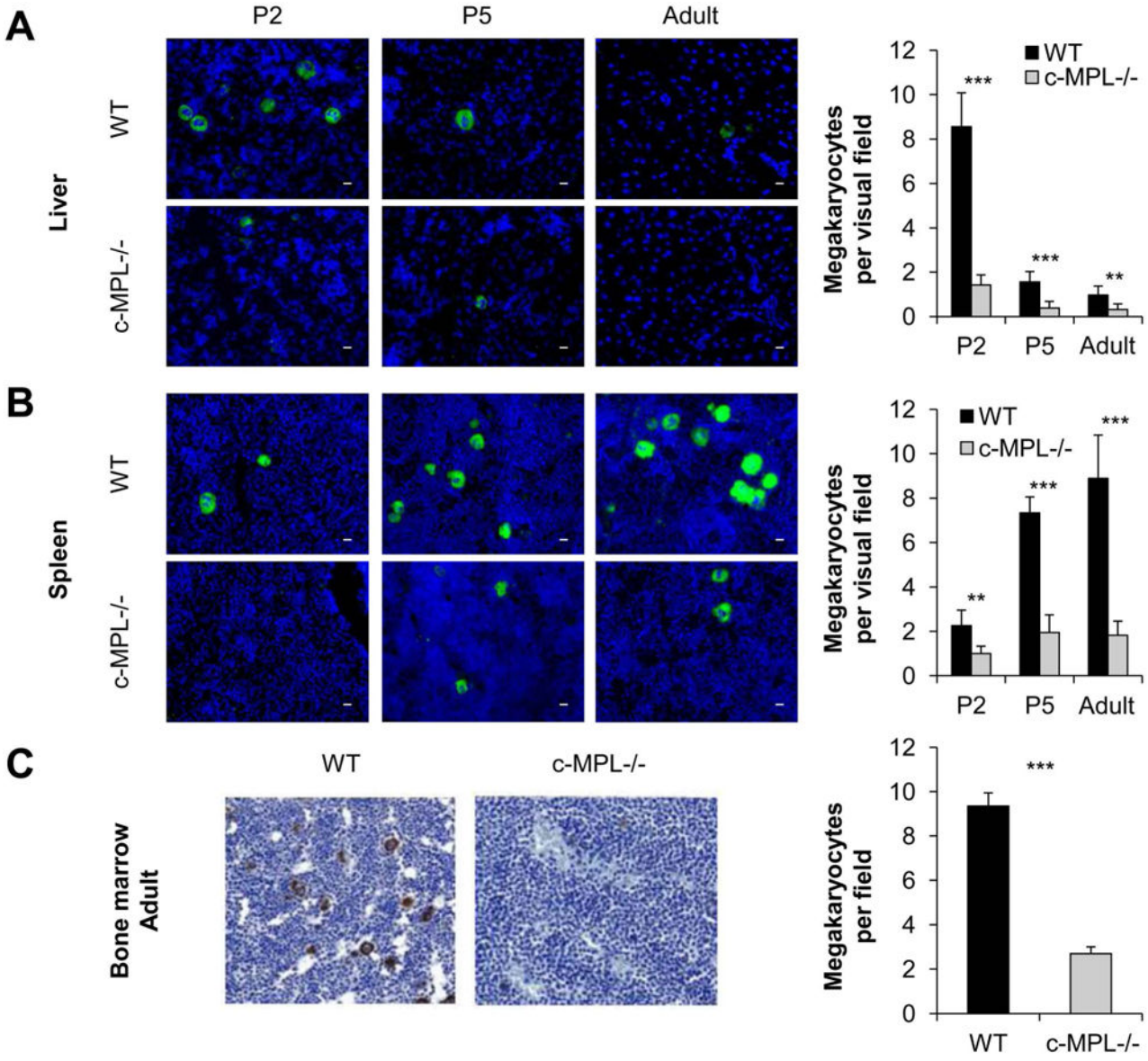

Figure 1. Liver and spleen MKs are reduced in *c-MPL*$^{-/-}$ newborn mice

(A, B) Liver and spleen samples were obtained from *c-MPL*$^{-/-}$ and WT mice at the indicated ages (P, post-natal day). Cryosections were fluorescently stained with anti-mouse GPIIb-FITC antibodies to detect MKs. Samples were photographed using a Nikon Eclipse fluorescent microscope equipped with a Nikon DXM1200F camera. Scale bar represents 10 μm. **(C)** Bone marrow samples obtained from adult WT and *c-MPL*$^{-/-}$ mice were immunohistochemically stained with vWF. Bars represent the mean ± SEM; n=5 mice per group; **P<0.01; ***P<0.001.

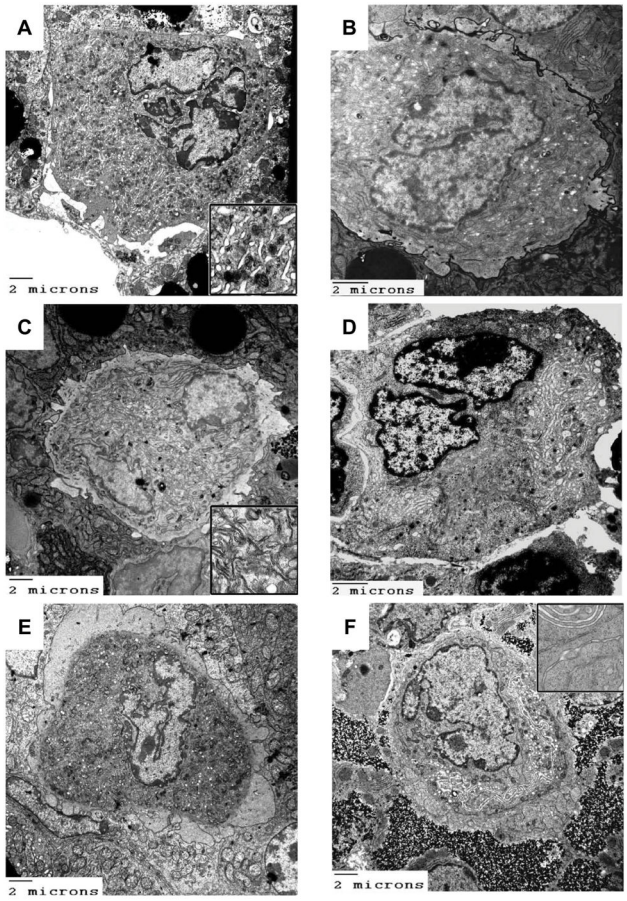

Figure 2. Bone marrow MKs in *c-MPL*$^{-/-}$ newborn mice display ultrastructural abnormalities

(A) Representative photomicrograph of a fully mature MK, with abundant granules and an open and well developed DMS distributed throughout the cytoplasm, found in the liver of a newborn WT mouse. **(B)** Immature neonatal *c-MPL*$^{-/-}$ MK, characterized by a large central nucleus with prominent nucleoli and a paucity of platelet granules in the cytoplasm. **(C)** Representative *c-MPL*$^{-/-}$ newborn liver MK showing a paucity of platelet granules and a poorly developed and disorganized DMS (see insert detail). **(D)** *c-MPL*$^{-/-}$newborn liver MK showing the DMS irregularly distributed throughout the cytoplasm. **(C, E, F)** Representative photomicrographs of *c-MPL*$^{-/-}$ newborn liver MKs exhibiting an abnormally wide peripheral zone, which did not contain any functional cellular material. All images were taken on a Tecnai G^2 Spirit Bio TWIN TEM (Hillsboro, OR) at an accelerating voltage of 80kV, and were recorded with an AMT 2k CCD camera (Danvers, MA). All inserts represent an area measuring 2 × 2 microns. Notice that *c-MPL*$^{-/-}$ MKs were significantly smaller than WT MKs.

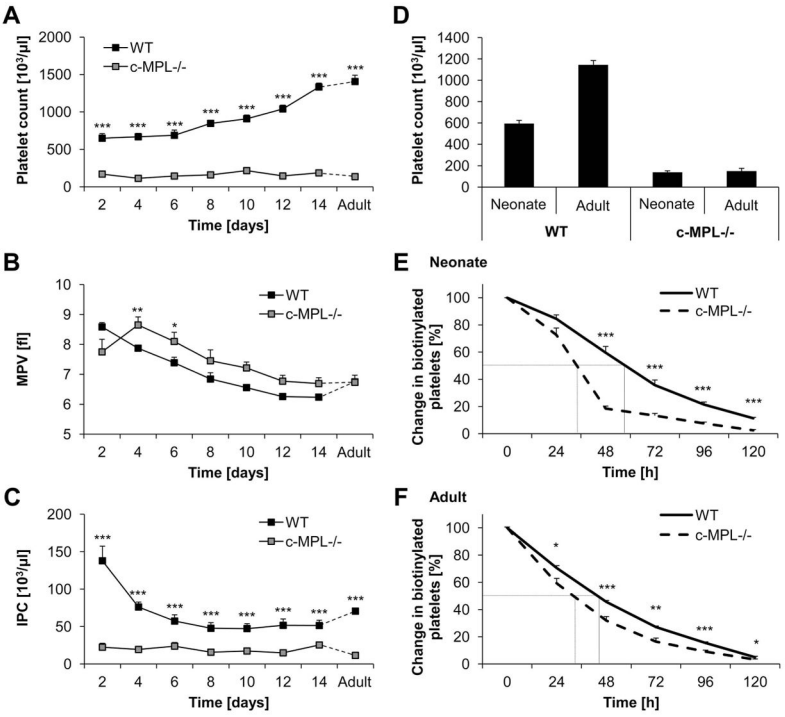

Figure 3. *c-MPL*$^{-/-}$ newborn platelets have a markedly reduced lifespan

(A, B, C) Platelet counts, MPV, and IPCs were quantified in *c-MPL*$^{-/-}$ and WT mice every other day between P2 and P14, and in adulthood. Results are mean ± SEM; n=5 mice per group; *P<0.05 **P<0.01; ***P<0.001. **(D, E, F)** Platelet counts were obtained before biotinylation (D). Platelet lifespan was evaluated by *in vivo* biotinylation in P2 (E) and adult (F) *c-MPL*$^{-/-}$ and WT mice, and the population of biotinylated platelets was monitored using flow cytometry. Lines indicate the times at which 50% of the platelets were gone (half-life). Results are mean ± SEM; n=6–8 mice per group; *P<0.05 **P<0.01; ***P<0.001.

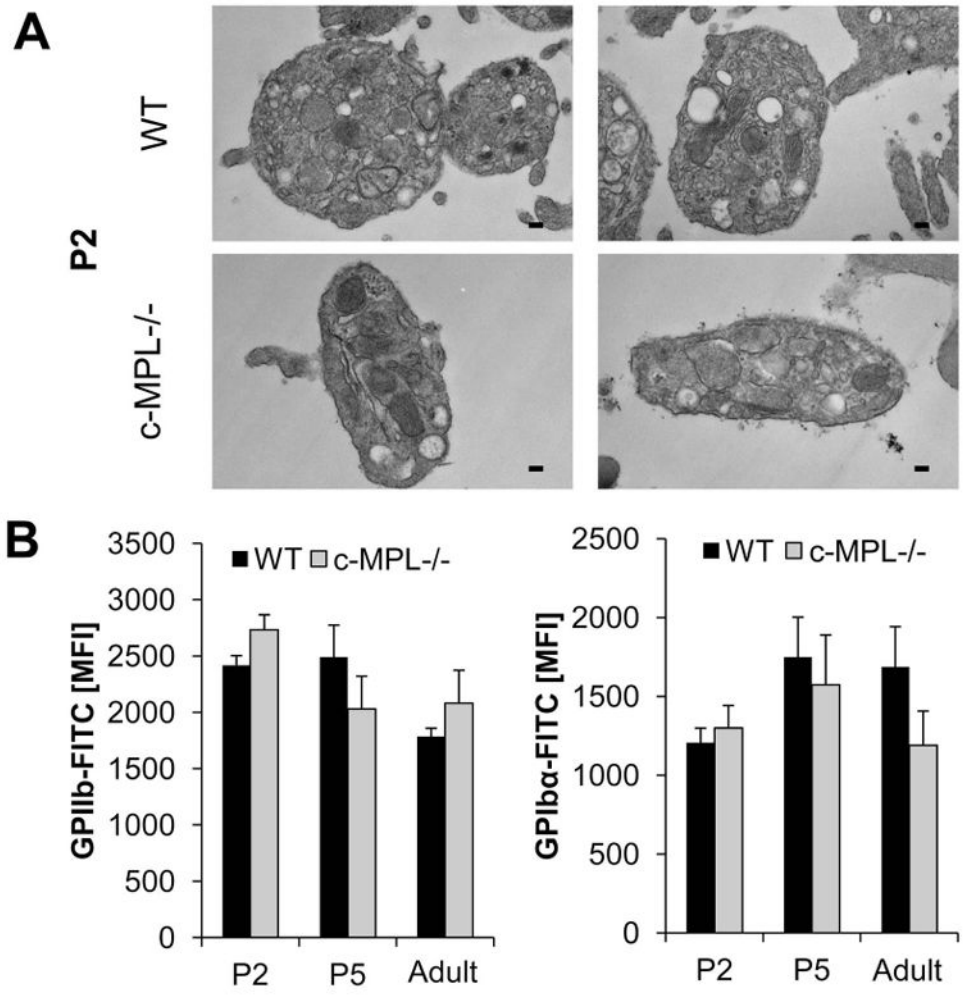

Figure 4. Platelets in *c-MPL*$^{-/-}$ newborn mice have normal morphology and surface glycoprotein expression

(A) Platelets from newborn (P2) *c-MPL*$^{-/-}$ and WT animals were isolated and the ultrastructure was studied by TEM. Scale bar represents 100 nm. N=3 mice per group. **(B)** Surface expression levels of GPIIb and GPIbα were measured by flow cytometry in *c-MPL*$^{-/-}$ and WT mice at the indicated post-natal age. Bars represent the mean ± SEM; n=6 mice per group.

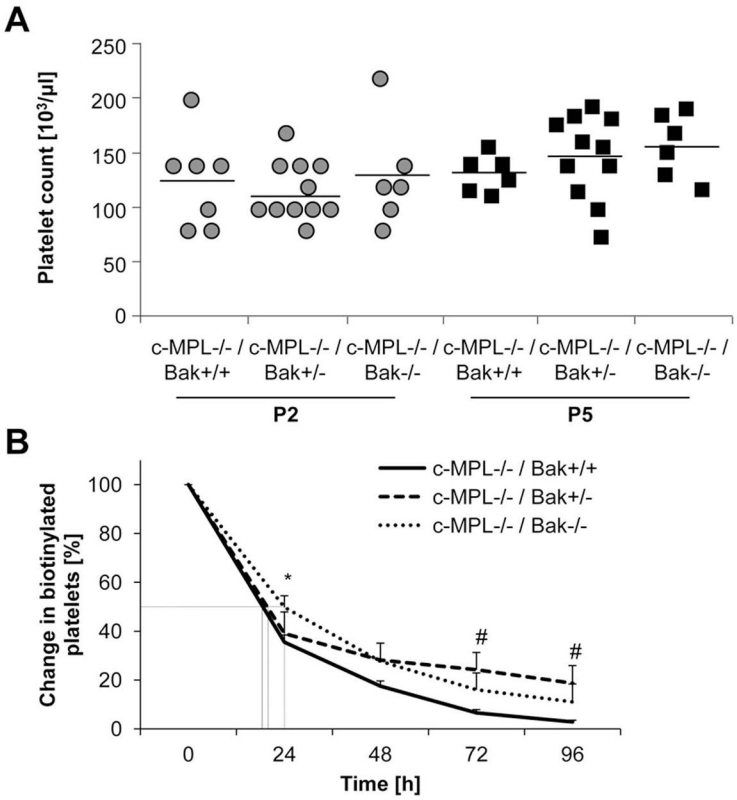

Figure 5. Reduced platelet half-life in *c-MPL*$^{-/-}$ mice is not corrected by Bak deletion

(A) Platelet counts from *c-MPL*$^{-/-}$/Bak$^{-/-}$, *c-MPL*$^{-/-}$/Bak$^{+/-}$, *c-MPL*$^{-/-}$/Bak$^{+/+}$ mice were measured at P2 and P5. **(B)** Platelet lifespan was evaluated by *in vivo* biotinylation in P2 *c-MPL*$^{-/-}$/Bak$^{-/-}$, *c-MPL*$^{-/-}$/Bak$^{+/-}$, and *c-MPL*$^{-/-}$/Bak$^{+/+}$ mice. Lines indicate the times at which 50% of the platelets were gone (half-life). Results are mean ± SEM; n=4–5 mice per group; * P<0.05 (*c-MPL*$^{-/-}$/Bak$^{+/+}$ vs. *c-MPL*$^{-/-}$/Bak$^{-/-}$); # P<0.05 (*c-MPL*$^{-/-}$ /Bak$^{+/+}$ vs. *c-MPL*$^{-/-}$/Bak$^{+/-}$).

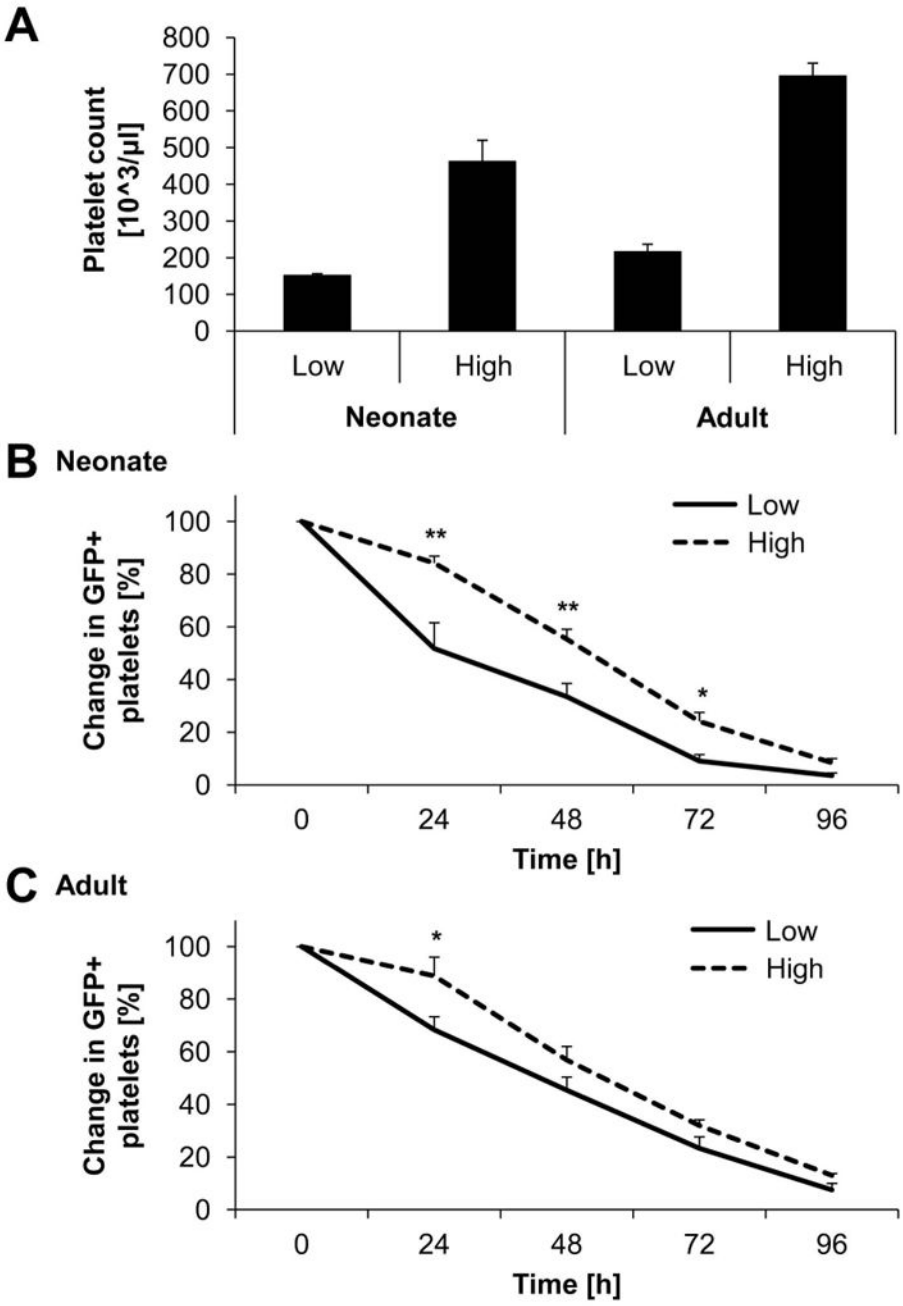

Figure 6. Transfused GFP+ platelets have a reduced lifespan in newborn *c-MPL*$^{-/-}$ mice

Platelets from adult GFP+ mice were isolated and injected into newborn P2 (**A and B**) or adult (**A and C**) *c-MPL*$^{-/-}$ mice at two different amounts (low and high). The post-transfusion platelet count was measured 2 h after the transfusion, and changes in the percentage of GFP+ platelets were followed for 96 hours. Results are mean ± SEM; n=5–9 in each group; *P<0.05 **P<0.01.

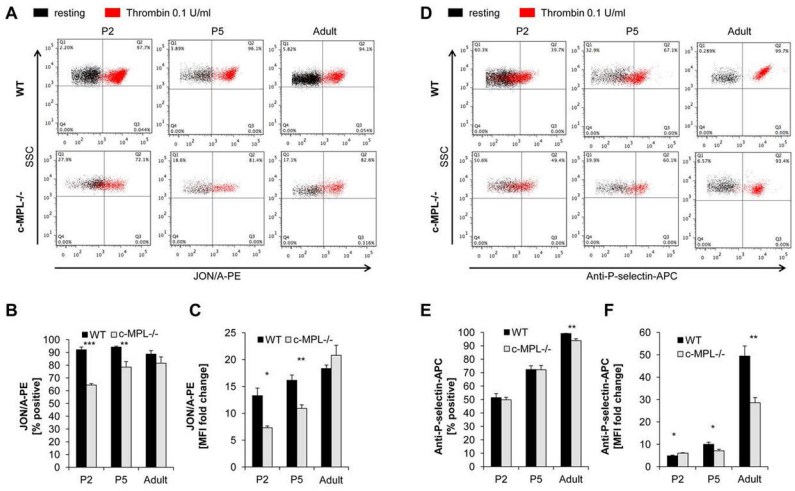

Figure 7. *C-MPL*$^{-/-}$ platelets have developmental stage- and genotype-specific platelet functional defects

To determine platelet activation, the surface expression levels of activated GPIIb/IIIa (binding of JON/A-PE, **A–C**) and P-selectin (**D–F**) were measured. Washed blood from WT and *c-MPL*$^{-/-}$ mice at the indicated post-natal ages was left untreated or incubated for 15 min with thrombin (0.1 U/ml) and analyzed by flow cytometry. Results are expressed as mean ± SEM; n=5–10 mice per group; * P<0.05, **P<0.01; ***P<0.001. **(A, D)** Representative dot plots for JON/A-PE and anti-P-selectin-APC expression in platelets from WT and *c-MPL*$^{-/-}$ mice at the indicated post-natal ages under resting or activated conditions. Results are shown as percentage of positive platelets **(B, E)** and MFI fold change between resting and activated platelets **(C, F)** following incubation with thrombin.